[Article ID] 1003- 6326(2002)01- 0071- 07

Erosion wear behaviour and mechanism of abradable seal coating①

RAN Li-ping(冉丽萍)
(State Key Laboratory for Powder Metallurgy, Central South University, Changsha 410083, China)

[Abstract] The erosion wear behaviour and mechanism of several middle temperature seal coatings were investigated by a CMS-100 self-made vacuum sand erosion machine. The results show that the relationship between the erosion mass loss and the erosion time is linear, the coatings hold a maximum erosion rate at 60° impact angle, and the relationship between the erosion rate and the impact speed is an exponential function. The speed exponent increases with the increase of the impact angle. At 90° impact, indentations and extruded lips were generated on the coating surface subjected to impact. With repetitive impact by the abrasive particles, the extruded lips were work-hardened and peeled off, while flattened metal phase grains were impacted repeatedly, loosed and debonded. At 30° impact, the erosion wear of the coating is characterized by micro-cutting, plowing and tunneling via pores and non-metal phase. The model of the erosion mechanism is advanced on the basis of the above-mentioned erosion wear behaviour.

[Key words] abradable seal coating; erosion wear; mechanism; model
[CLC number] TG 115.5 [Document code] A

1 INTRODUCTION

The clearance between the rotating blades and the casing should be as small as possible in order to increase the efficiency and reduce the fuel consumption of an aircraft turbine engine[1]. The gas path sealing has become an important method for this purpose[2]. The thermal sprayed abradable seal coating has been used because of its simple manufacturing processes, easy repair of the components, easy adjustment of its properties and good sealing effectiveness[2]. Also, it can provide thermal barrier for the casing, and reduce the influence of the high temperature fuel gas on the casing[2,3]. The coating is a kind of composite material composed of metal phase and self-lubricating non-metal phase with many pores[4]. In application, it is required that the rotor blades scrape the coating to form a minimum clearance. So the coating should be not only soft enough to be easily scraped without damaging the blades—good abradability, but also hard enough to resist against the erosion by the high speed gas flow and the solid particles in the gas—good erosion resistance[3~6]. The abradability and erosion resistance are the most important properties of the coating. However, the two are contradictory[5,6]. Thus the coating should provide a good balance between the abradability and the erosion resistance.

The researchers and users have paid attention to the study[5~9] of the powders, spray processes, properties of the coating and the relationship among them. However, the basic researches about the abradability and the erosion resistance have not been well-made[4,10,11]. Especially, the research about the erosion wear behaviour of the coatings has not been much reported. Because of high porosity and much non-metal phase in the coating, its erosion wear rule and behaviour can be different from those of bulk material and some coatings. So it is imperative to study its rule and behaviour. In this paper the erosion wear rule and mechanism of several middle temperature abradable seal coatings are investigated, and the model of the erosion wear is advanced.

2 EXPERIMENTAL

The sprayed powders were METCO 307 (75% Ni+ 25% graphite G), METCO 310 (57% Al+ 8% Si+ 35% G), METCO 313 (40% Al+ 5.5% Si+ 45.5% G+ 9% organic binder) and METCO 601 (40% polyester+ 60% Al-Si alloy), which were made by METCO, USA. The sprayed coating specimens were called as M307, M310, M313 and M601, respectively. Four kinds of powders made in China, which were slightly different from the corresponding METCO powders in composition, were also used. The coating specimens prepared by the powders made in China were called as F307, F310, F313 and F601, respectively. M307 and F307 were classified as 307 type of coating, and the other classified in a similar way. M307, F307, M310 and F310 coatings were sprayed on the blasted surface of low carbon steel plate by a METCO-6P flame spray system. M313, F313, M601 and F601coatings were sprayed by a METCO-7MB plasma spray system. Specimens with

① [Foundation item] Project supported by the National Defense Science and Technology Pre-research Foundation of China
[Received date] 2001- 02- 08; [Accepted date] 2001- 09- 05

different microstructure and hardness were prepared for each kind of powder by changing spray parameters. The microstructure and hardness of the coating specimens are listed in Table 1. Fig. 1 shows the microstructure of the cross section of M310-2 coating, where the white matrix is AlSi alloy, the grey phase is graphite, the black phase is pore.

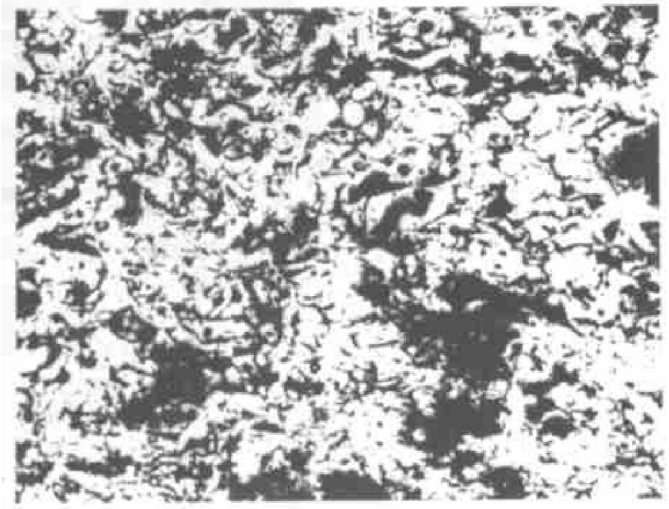

Fig. 1 Microstructure of cross section of M310-2 coating

Table 1 Microstructure and hardness of coating specimens

Specimen	Metal phase/ %	Non-metal phase/ %	Porosity / %	HR15y
M307-1	43.7	25.9	30.4	18
M307-2	46.8	26.0	27.2	20
M307-3	53.6	27.3	19.1	60
F307-1	35.3	31.6	33.1	- 52
F307-2	39.1	28.3	32.6	- 34
F307-3	46.6	26.1	27.3	- 20
M301-1	43.9	20.4	35.7	- 12
M301-2	62.9	14.5	7.6	28
F301-1	82.5	13.0	4.5	73
F310-2	78.8	16.5	4.7	57
M313-1	74.0	18.3	7.7	74
M313-2	70.1	21.8	8.1	70
M313-3	74.9	17.9	7.2	77
F313	62.7	26.0	11.3	57
M601-1	29.4	69.3	1.3	51
M601-2	34.1	65.2	1.7	53
F601	53.9	44.6	1.5	65

Erosion wear test was made on a CMS-100 self-made erosion machine. Fig. 2 shows the schematic diagram of the machine. The specimens to be tested

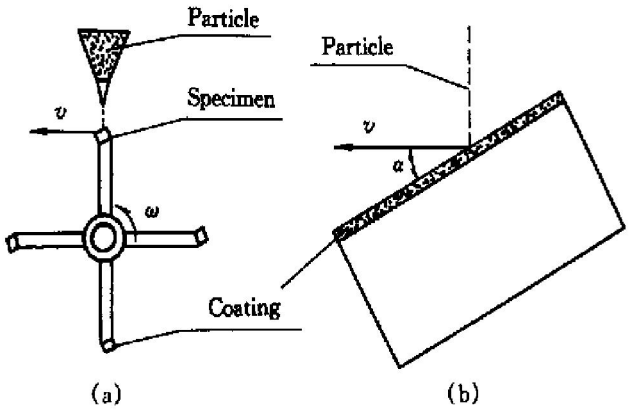

Fig. 2 Schematic diagram of erosion tester (a) and specimen (b)

and abrasive particle were held in a 1.3~ 6.5 Pa vacuum chamber. The abrasive particle was 147 μm corundum whose feeding rate was 16 g/ min. The impact angles were 30°, 60° and 90°. Because the mean velocity of 0.15~ 0.30 mm diameter solid particles in the gas flow with 150 m/ s velocity was 30 ~ 70 m/ s[12], the impact test speeds were 20~ 80 m/ s which is the linear velocity of the rotary specimens. Erosion time was 1 h, but the time and impact speed were changed for some specimens. The ratio of the mass loss of the specimen to the mass of the grit, E, was recorded as the erosion rate.

3 RESULTS AND DISCUSSION

3.1 Rule of erosion wear

3.1.1 Effect of erosion time

The relationship between the mass loss and the erosion time at given impact angles is linear, as shown in Fig. 3. This indicates that the erosion rate of the coatings is not related to the erosion time under the same erosion condition, such as impact angle, erosion speed, the kind and size of abrasive particles.

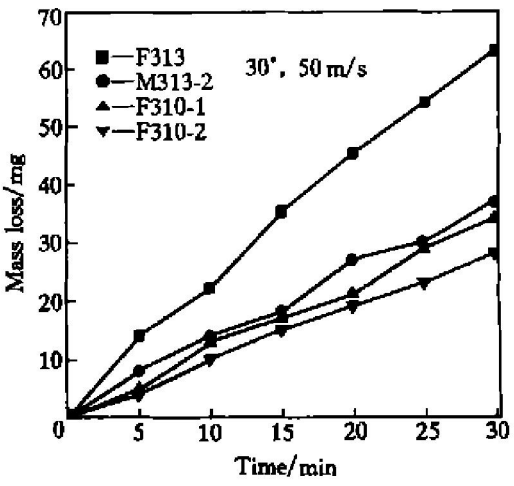

Fig. 3 Erosion mass loss vs impact time

Meanwhile, the relationship indicates that the erosion rate of the coatings is related to the characteristics of the coating type, microstructure and hardness, but independent on the thickness of the coatings. Therefore, the erosion rate can act as a basis of the design of coating lifetime under the given systematic parameters.

Bulk materials and some coatings have an erosion inoculation period, that is, the mass loss does not occur immediately at the initial impact[13,14]. Only if the strain caused by impinging particles accumulates to a critical value, can the metal grains on the impacted surface of the materials fall off and the mass loss appear, and then the erosion rate transits gradually to a stable state. However, the erosion rate of the abradable seal coatings at the initial stage becomes a stable state, which is related to the high porosity, large volume fraction of non-metal phase and weak adhesion between metal grains in the coatings. This is peculiar to the erosion wear of the abradable seal coatings.

3.1.2 Effect of impact angle

Fig. 4 shows the erosion rate vs impact angle. It is seen that the erosion rate of all the tested specimens comes to the maximum at an impact angle 60°.

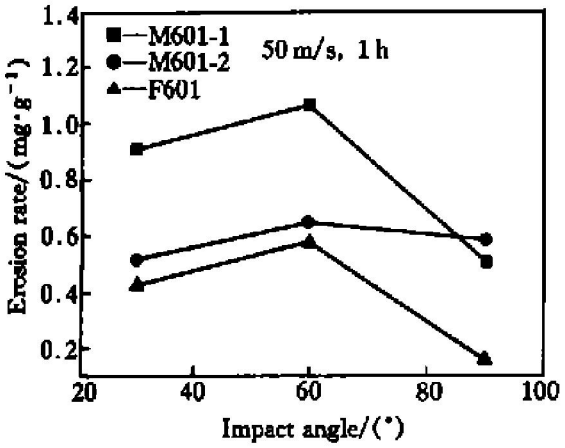

Fig. 4 Effect of impact angle on erosion rate

According to the common rule of the erosion rate with the change of impact angle α, the erosion wear can be divided into plastic material wear and brittle material wear. The relationship[13] between erosion rate and impact angle can be expressed as

$$E = A\cos^2\alpha\sin m\alpha + B\sin^2\alpha \quad (1)$$

where m, A and B are constants. For typical brittle material, A is equal to zero and the erosion rate is largest at 90° impact angle. For typical plastic material, B is equal to zero and the erosion rate is largest at 20~ 30° impact angle. Therefore, the erosion behaviour of the abradable seal coating lies between the behaviour of the plastic material and that of the brittle material.

Because the hardness of the seal coatings, in which the metal phase resisting erosion wear is typical plastic material, is very low, the erosion wear is mainly micro-cutting and plowing at low impact angle. On the other hand, because the normal impact on the surface of the coating increases with the increase of impact angle, and because the coatings are of high porosity and weak adhesion between the metal phase grains and the non-metal phase, which are like cracks, the erosion wear of the coating at larger impacting angle could behave similar to that of brittle materials. Therefore, the erosion rate of the coating is largest at 60° impact angle.

3.1.3 Effect of impact speed

Fig. 5 shows the relationship between the erosion rate E and the impact speed v at 30° impact angle. According to regression analysis, we have

$$E = Cv^n \quad (2)$$

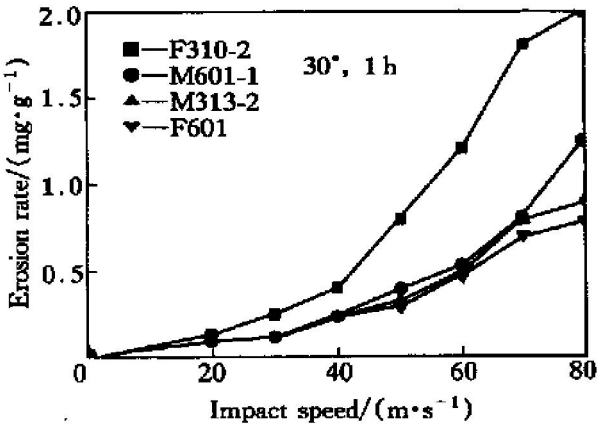

Fig. 5 Effect of impact speed on erosion rate

where C is a constant, n is a speed exponent. Table 2 lists C and n values at different impact angles. Table 2 indicates that the speed exponent depends on the impact angle. The different exponents result from different erosion wear mechanisms of the coatings at different impact angles. Moreover, n increases with the increase of impact angle, showing that the increase of impact speed results in the remarkable increase of the erosion rate. The maximum erosion mass loss moves to a higher impact angle with the increase of impact speed. Therefore, the erosion of the coatings at larger impact angles resembles to that of a brittle material. At a low impact angle, the speed exponent of the coating is close to that of plastic material. However, at impact angles 60° and 90°, the exponent n is larger than that of brittle material[13].

3.2 Erosion wear mechanism and model

Fig. 6(a), (b) show respectively the surface morphologies of F601, M313-2 coatings impacted at 90°, 50 m/s. The indentations and extruded lips on the surface of the metal phase in the coatings are clearly seen in the figures. The adhesion between some lips and the metal phase matrix is weak, and the lips could be easily peeled off by repeated impact.

Table 2 Results of regression analysis of relationship between erosion rate and impact speed

Specimen	30°		60°		90°	
	$C/10^{-4}$	n	$C/10^{-6}$	n	$C/10^{-6}$	n
F310-2	1.7	2.01	7.88	2.81	3.41	3.01
M313-2	1.34	2.04	9.59	2.86	3.84	3.02
M601-1	2.98	2.02	6.69	3.00	2.25	3.22
F601	1.63	1.96	6.35	2.83	4.03	2.96

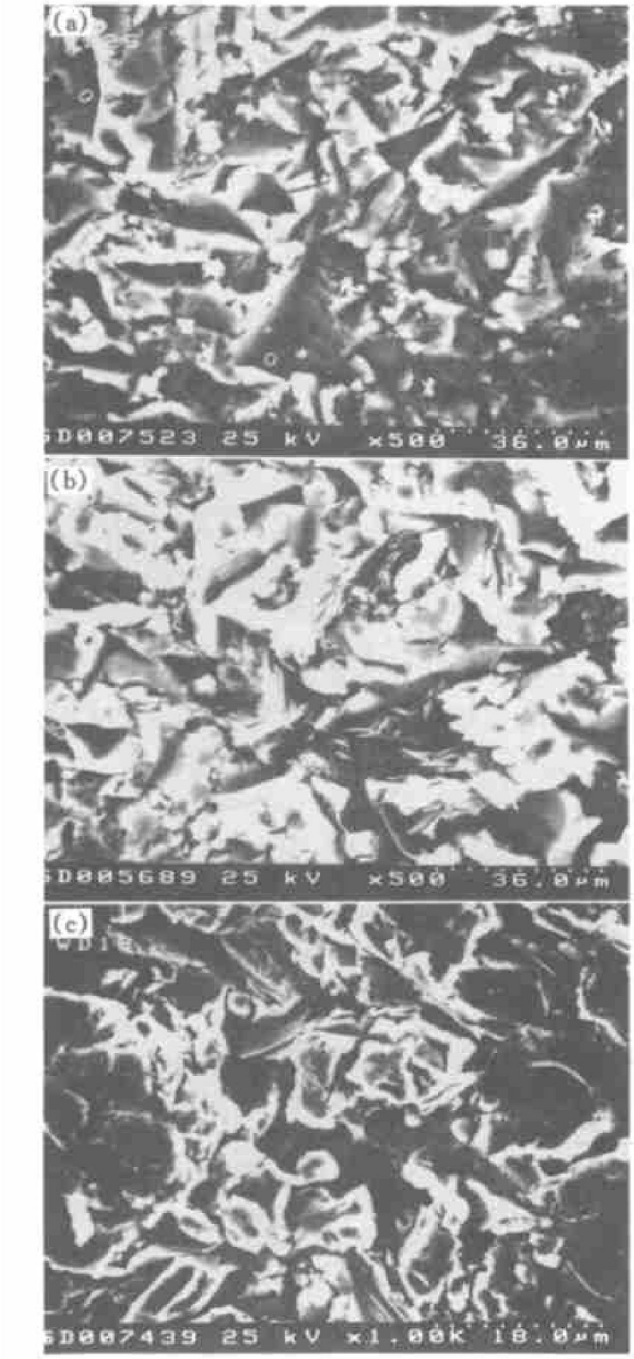

Fig. 6 Surface morphologies of F601 (a), M313-2(b), M307-3(c) coatings impacted at 90° and 50 m/s

Therefore, it is thought that at 90° impact angle, the abrasive particles impact on the surface of the metal phase in the coating and produce indentations and extruded lips, and then the lips impacted repeatedly by abrasive particles become work-hardened and eventually fall off.

Since the coatings have many pores and a large volume fraction of non-metal phase, which are like pre-cracks, the metal grains in the coating are separated by the pores and non-metal phase and become a non-continuous body. Subsequently the adhesion between the metal grains is weak. During normal impacting of the abrasive particles, the surface of the coating endures Hertz force and experience partial plastic deformation, accompanied by initiation of cracks. The cracks propagate through the grain boundaries, and then the flattened metal grains on the coating surface become loose and eventually fall off by repeated impact, as shown in Fig. 7.

Fig. 6(c) shows the surface morphology of M307-3 coating impacted at 90° impact angle. It is clearly seen that the indentation effect for 307 coating at 90° is not so remarkable as that for 310, 313 and 601 coatings. The reason is that the hardness of the metal phase in 307 coating is higher than that in 310, 313 and 601 coatings. In addition, the flattened metal grains easily fall off after a few impacts, because 307 coatings have higher porosity, a larger volume fraction of non-metal phase and weaker adhesion between the metal grains. The feature of extruded lips on the surface of 307 coating is not remarkable, because the debond of the flattened metal grain occurs prior to the generation of the extruded lips in repetitive impact.

Fig. 8(a), (b) show the eroded surface morphologies of M313, M601 coating impacted at 90°, 50 m/s respectively. The pictures indicate that the graphite in the coatings is impacted and fell off prior to metal phase, leaving caves; but the polyester in 601 coating stays longer than the graphite in the other coatings because it can endure high elastic strain and absorb impact energy of the abrasive particles. With the removal of the graphite, 307 coating becomes loose, porous and honeycomb-like. This indicates that the erosion resistance of the graphite in the coatings is extremely poor and the polyester in 601 coating has good erosion resistance.

The erosion wear mechanism of the abradable seal coating at 90° impact can be expressed as below: 1) the abrasive particles impact and extrude the surface of the coating, and produce indentations and extruded lips, accompanied by the peeling off of the lips; 2) the flattened metal phase grains in the surface layer of the coating be loosened and de-bonded by repeated impact. The former effect is more remarkable for 310, 313 and 601 coatings, and the latter effect is more remarkable for 307 coating. To summarize, the model of indentation and delamination of grains for the abradable seal coating at 90° impact angle is put forward and shown in Fig. 9(a).

Fig. 10(a), (b) and (c) show respectively the surface morphologies of erosion worn F313, M601-1 and M307-3 coatings impacted at 30°, 50 m/s. Micro-cutting and plowing traces, and curled parts produced by cutting and plowing are observed in the figures. Cracks occur between the curled parts and the metal phase matrix. The curled parts are repeatedly impacted by impinging particles and easily fall off. This indicates that the micro-cutting and plowing caused by shear component of the abrasive particles play a dominant role at lower impact angle. Fig. 10(b) shows also that the micro-cutting and plowing traces on the eroded surface of 601 coating are short, shallow and flat, because the polyester in

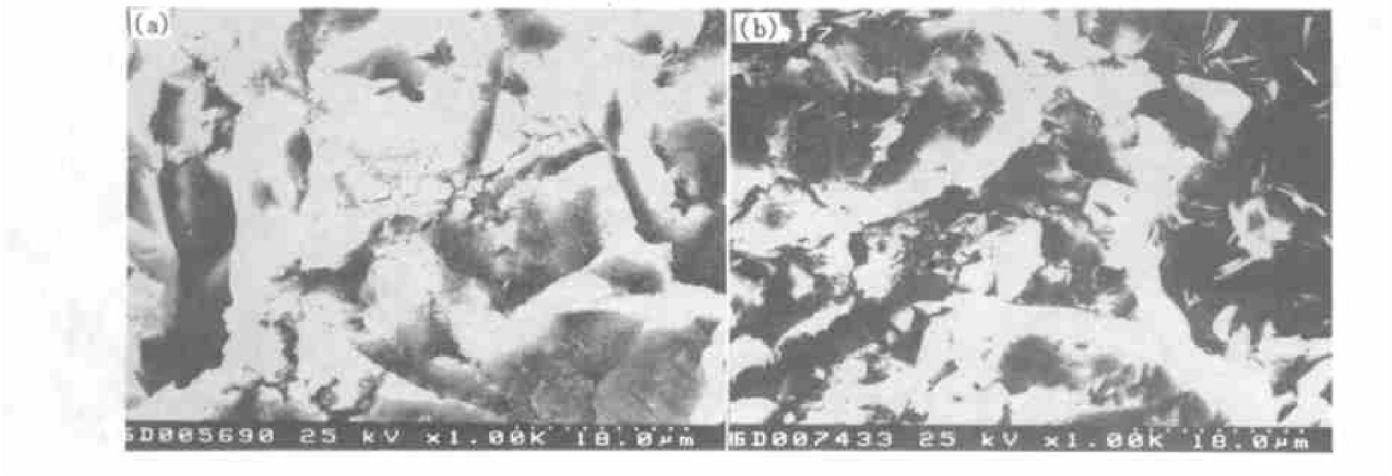

Fig. 7 Cracks on surfaces of F313 coating (a) and loosened metal phase grain of M313-2 coating (b) impacted at 90° and 50 m/s

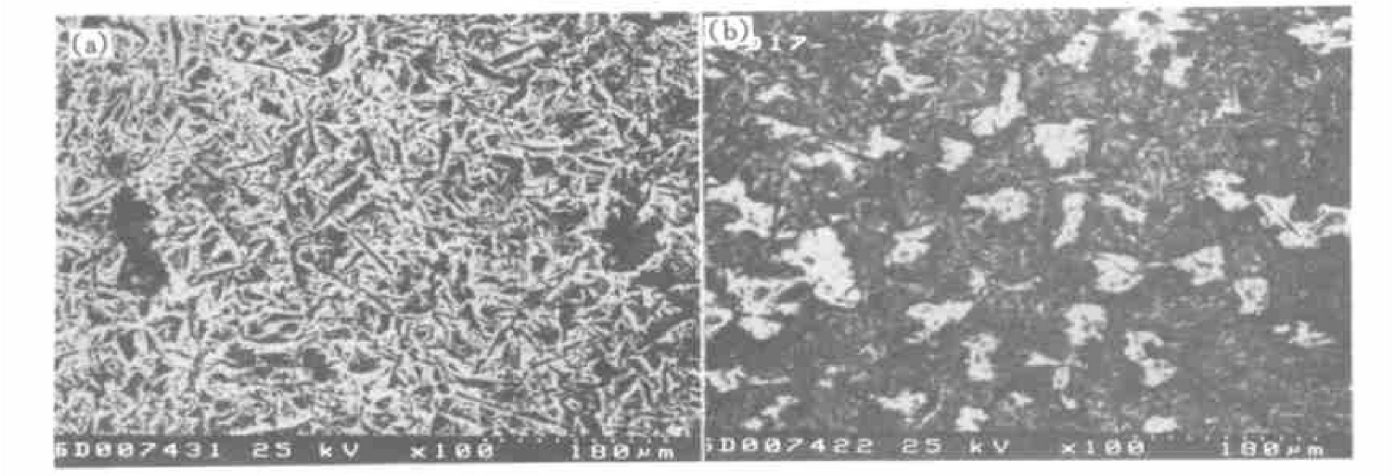

Fig. 8 Surface morphologies of M313 (a) and M601 (b) coating impacted at 90° and 50 m/s

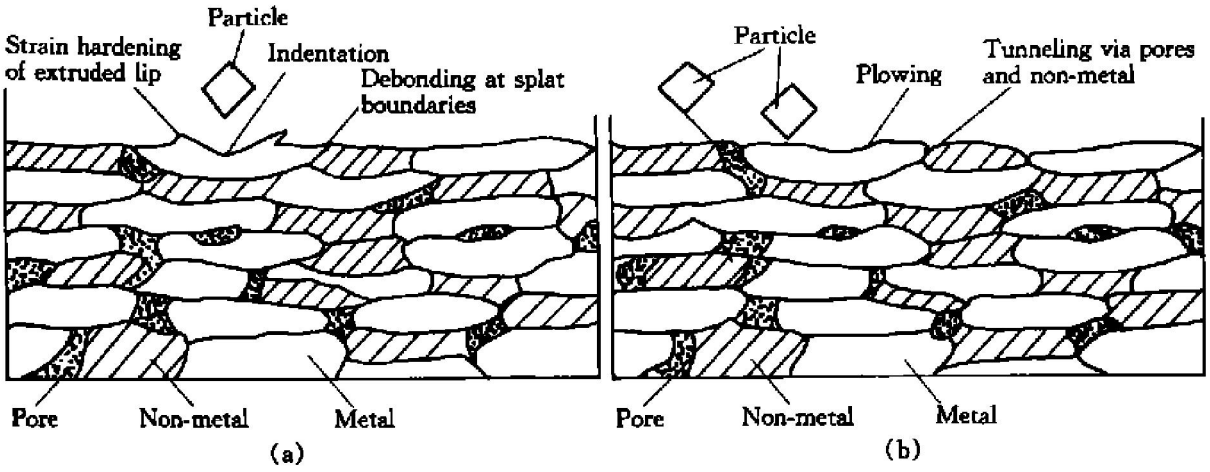

Fig. 9 Model of erosion wear at 90° (a) and 30° (b)

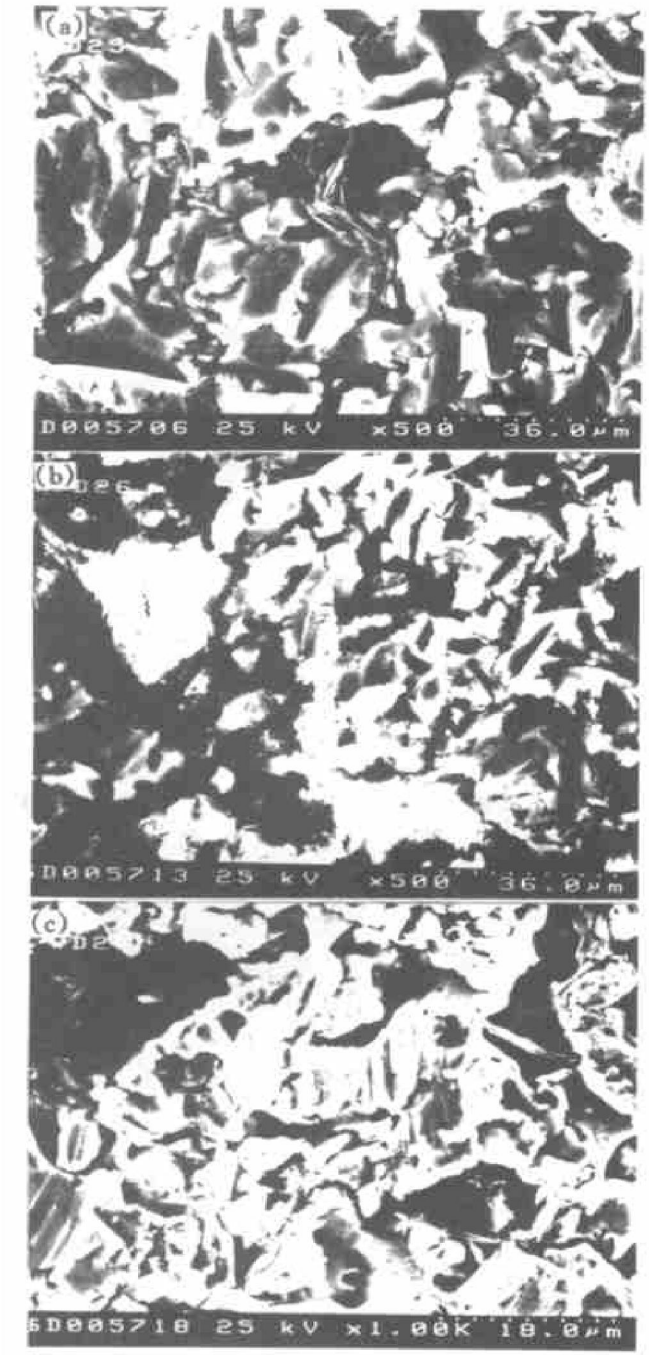

Fig. 10 Surface morphologies of F313 (a), M601-1 (b) and M307-3 (c) coating impacted at 30° and 50 m/s

the coating absorbs partial energy of the impinging particles. Compared with 310, 313 and 601 coatings, the micro-cutting and plowing traces in 307 coating are shorter, more shallow and flatter, and the amount of curled parts is less, as shown in Fig. 10(c). This is attributed to the higher hardness of metal phase Ni, higher porosity and larger amount of non-metal phase in 307 coating. In addition, in the presence of high porosity and a large volume fraction of non-metal phase, the impinging particles produce tunneling via pores and non-metal phase during micro-cutting and plowing. This process accelerates the mass loss of the coating. The tunneling is more remarkable in 307 coating. Therefore, the erosion wear of the abradable seal coating at 30° impact angle is characterized by micro-cutting, plowing and tunneling via pores and non-metal phase, as shown in Fig. 9(b).

Fig. 11 shows the eroded surface morphology of F313 coating impacted at 60° and 50 m/s. It is clearly seen that the traces of micro-cutting and plowing are not so shallow and flat as those at 30°, and the indentation and extruded lips are not so remarkable as those at 90°. Thus, the erosion wear of the coatings at 60° lies between that at 30° and that at 90°.

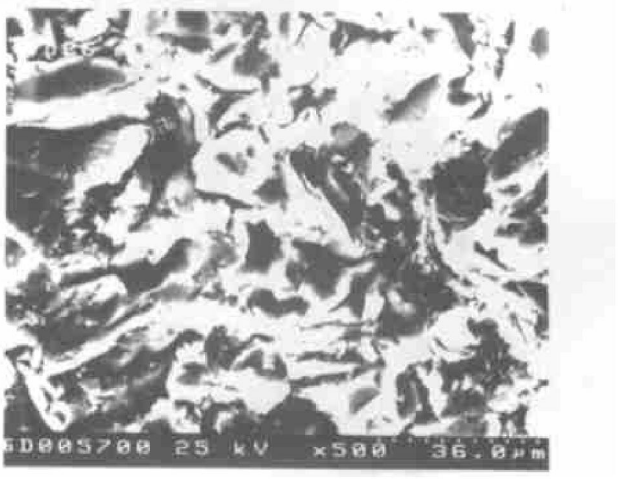

Fig. 11 Surface morphology of F313 coating impacted at 60° and 50 m/s

4 CONCLUSIONS

1) The relationship between erosion wear mass loss of the abradable seal coatings and erosion time is linear, and no erosion inoculation period is observed. The coatings hold a maximum erosion rate at 60° impact angle. The relation between erosion rate and impact speed is an exponential function. The speed exponent increases with the increase of impact angle.

2) At 90° impact angle, the abrasive particles impact and extrude the surface of the coatings, and produce indentations and extruded lips, and then the lips become work-hardened by repeated impact and eventually fall off. The flattened metal phase grains in the surface layer of the coating loosen and de-bond by repeated impact. The former effect is more remarkable for 310, 313 and 601 coatings, and the latter effect is more remarkable for 307 coating. The erosion resistance of the graphite in the coatings is extremely poor and is eroded away prior to the metal phase.

3) At 30° impact angle, the erosion wear of the coatings is characterized by micro-cutting, plowing and tunneling via pores and non-metal phase. Erosion wear at 60° lies between that at 30° and that at 90°.

[REFERENCES]

[1] Demasi J T. Protective coating in the gas turbine engine [J]. Surf Coat Technol, 1994, 68- 69: 1- 9.

[2] Novinski E R. The design of thermal sprayed abradable seal coatings for gas turbine engines [A]. Proceedings of 4th National Thermal Spray Conference [C]. USA, 1991. 451- 454.

[3] YI Mao-zhong. Friction and wear behaviour and abradability of abradable seal coating [J]. Wear, 1999, 231: 47- 53.

[4] Oka T. Basic characteristic of different abradable coatings [A]. Proceedings of International Thermal Spraying Conference [C]. Germany, 1990. 58- 67.

[5] Novinski E R. Process parameter impact on the physical properties of an advanced abradable coating [A]. Proceedings of 3rd National Thermal Spray Conference [C]. USA, 1990. 151- 157.

[6] YI Mao-zhong, ZHANG Xian-long, JI Geng-shun, et al. Erosion wear of AlSi-graphite and Ni/graphite abradable seal coating [J]. Trans Nonferrous Met Soc China, 1997, 7(2): 99- 102.

[7] Dorfman M. A high performance alternative to NiCrAl/bentonite for gas turbine abradable seals [A]. Proceedings of 13th International Thermal Spray Conference [C]. USA, 1992. 587- 594.

[8] Chon T. Aluminium-silicon/polyester abradable coatings [A]. Proceedings of 3rd National Thermal Spray Conference [C]. USA, 1990. 625- 630.

[9] Ghasripoorf F, Schmicl R K. A review of clearance control wear mechanisms for low temperature aluminium silicon alloys [A]. Proceedings of the 15th International Thermal Spray Conference [C]. France, 1998, 139- 144.

[10] Knuuttila J, Ahmanieni S. Wet abrasion and slurry erosion resistance of sealed oxide coatings [A]. Proceedings of the 15th International Thermal Spray Conference [C], France, 1998, 145- 150.

[11] YI Mao-zhong. Evaluation of Al-Si/polyester abradable seal coating [J]. Trans Nonferrous Met Soc China, 1996, 6(4): 110- 113.

[12] Tabakoff W. Investigation of coatings at high temperature for use in turbomachinery [J]. Surf Coat Techn, 1989, 40: 97- 115.

[13] LI Shi-zhou, DONG Xiang-lin. Erosion Wear and Fretting Wear of Materials [M], (in Chinese). Beijing: Mechanical Industry Press, 1987.

[14] Tilly G P. The interaction of particle and material behaviour in erosion processes [J]. Wear, 1970, 16: 447 - 450.

(Edited by YUAN Sai-qian)